

ORIGINAL ARTICLE

Air–water oxygen exchange in a large whitewater river

Robert O. Hall Jr.,¹ Theodore A. Kennedy,² and Emma J. Rosi-Marshall^{3,4}**Abstract**

Air–water gas exchange governs fluxes of gas into and out of aquatic ecosystems. Knowing this flux is necessary to calculate gas budgets (i.e., O₂) to estimate whole-ecosystem metabolism and basin-scale carbon budgets. Empirical data on rates of gas exchange for streams, estuaries, and oceans are readily available. However, there are few data from large rivers and no data from whitewater rapids. We measured gas transfer velocity in the Colorado River, Grand Canyon, as decline in O₂ saturation deficit, 7 times in a 28-km segment spanning 7 rapids. The O₂ saturation deficit exists because of hypolimnetic discharge from Glen Canyon Dam, located 25 km upriver from Lees Ferry. Gas transfer velocity (k_{600}) increased with slope of the immediate reach. k_{600} was $< 10 \text{ cm h}^{-1}$ in flat reaches, while k_{600} for the steepest rapid ranged 3600–7700 cm h^{-1} , an extremely high value of k_{600} . Using the rate of gas exchange per unit length of water surface elevation (K_{drop} , m^{-1}), segment-integrated k_{600} varied between 74 and 101 cm h^{-1} . Using K_{drop} we scaled k_{600} to the remainder of the Colorado River in Grand Canyon. At the scale corresponding to the segment length where 80% of the O₂ exchanged with the atmosphere (mean length = 26.1 km), k_{600} varied 4.5-fold between 56 and 272 cm h^{-1} with a mean of 113 cm h^{-1} . Gas transfer velocity for the Colorado River was higher than those from other aquatic ecosystems because of large rapids. Our approach of scaling k_{600} based on K_{drop} allows comparing gas transfer velocity across rivers with spatially heterogeneous morphology.

Keywords: Colorado River, gas transfer velocity, Grand Canyon, rapids, reaeration, river geomorphology

Introduction

[1] Air–water gas exchange governs the flux of atmospheric gases into and out of aquatic ecosystems. Measurements of gas flux are needed for estimating rates of whole-ecosystem metabolism (Odum 1956) or basin-scale carbon budgets (Cole et al. 2007). Gas flux is calculated as the gas concentration gradient between water and air multiplied by a gas transfer velocity. Gas transfer velocity has been measured in many aquatic ecosystems by adding a deliberate tracer gas (e.g., propane or SF₆), whose evasion is then measured through

time in lakes (Cole and Caraco 1998), oceans (Wanninkhof et al. 1993), estuaries (Clark et al. 1994), rivers (Caplow et al. 2004), and small streams (Wanninkhof et al. 1990; Melching and Flores 1999). Other approaches for estimating gas transfer velocity include measuring flux within a floating dome (Marino and Howarth 1993; Kremer et al. 2003) and predicting flux based on measured turbulence (Zappa et al. 2007). Relative to other aquatic ecosystems, large rivers have fewer measures of gas exchange (Raymond and Cole 2001), with the Hudson River being a notable exception

¹Department of Zoology and Physiology, University of Wyoming, Laramie, Wyoming 82071, USA

²Southwest Biological Science Center, United States Geological Survey, Flagstaff, Arizona 86001, USA

³Department of Biology, Loyola University Chicago, Chicago, Illinois 60626, USA

⁴Current address: Cary Institute of Ecosystem Studies, Millbrook, New York 12545, USA

Correspondence to
Robert O. Hall Jr.,
bhall@uwyo.edu

(Clark et al. 1994; Ho et al. 2011). A review of 493 gas tracer experiments contained only 25 (5%) measurements from rivers with discharge $> 10 \text{ m}^3 \text{ s}^{-1}$, and only one $> 100 \text{ m}^3 \text{ s}^{-1}$ (Melching and Flores 1999). Recent measures using domes have provided many new estimates for low-gradient rivers (Alin et al. 2011).

[2] Many large rivers have a relatively unbroken water surface and thus are similar to lakes and estuaries where wind speed and turbulence due to currents drive gas exchange (Borges et al. 2004; Alin et al. 2011; Ho et al. 2011). In these smooth-surface water bodies, established wind speed–gas exchange relationships can constrain estimates of gas transfer velocity. However, many large rivers have riffles and rapids, thus mimicking small streams where geomorphology and current velocity regulate gas exchange (Melching and Flores 1999; Mulholland et al. 2001). Without validation, it is unreasonable to use the statistical and mechanistic models developed for small streams to estimate gas transfer velocity on large rivers. Further, despite good fits of empirical models to data, statistically predicted versus actual gas exchange rates from tracer studies can vary 5-fold (Melching and Flores 1999), which is too uncertain to accurately estimate gas flux for the purposes of whole-ecosystem metabolism estimates. Mulholland et al. (2001) showed that mechanistic equations poorly predicted measured rates of gas transfer in small streams. Hence, empirical measurements are needed to calculate gas flux from rivers with substantial riffles and rapids. Dome methods (Kremer et al. 2003) and those that measure water turbulence (e.g., Zappa et al. 2007) would be difficult to apply in these types of rivers because of the extreme difficulty in floating domes or measuring surface turbulence through large rapids. In addition, scaling these estimates to a spatially variable river would be tenuous. Therefore, measuring gas transfer velocity in such rivers would require either a tracer addition or measuring the change in concentration of a naturally occurring gas that is far from saturation (e.g., a river with a large dam that releases low-oxygen hypolimnetic water).

[3] Here we measured gas exchange in a 28-km segment of the Colorado River, Grand Canyon, with large rapids below a hypolimnetic release dam. We measured invasion of O_2 into low- O_2 water that emerges

from Glen Canyon Dam. We hypothesized that rapids would have high rates of gas exchange relative to flat sections. Thus, slope drives gas transfer velocity.

Methods

[4] The Colorado River downstream of Glen Canyon Dam (average discharge, Q , $325 \text{ m}^3 \text{ s}^{-1}$) is a 466-km-long tailwater extending to Lake Mead, the reservoir formed by Hoover Dam. For the first 25 km below the Glen Canyon Dam (Glen Canyon reach) the river has no rapids. Below Lees Ferry (Arizona), which marks the end of Glen Canyon, the river enters Grand Canyon National Park, where the river morphology changes to a series of pools and runs punctuated by > 150 rapids that account for most of the elevation loss between Lees Ferry and Lake Mead (Leopold 1969). Rapids are located at debris fans associated with tributary inputs in areas of bedrock fractures (Dolan et al. 1978). Our study segment was the first 28 km downstream of Lees Ferry (latitude 36.88°N , longitude 111.60°W) because this segment has low- O_2 water released from Glen Canyon Dam. Rapids range from small riffles, for example, Cathedral Wash (slope = 0.0045, elevation drop = 0.4 m), to House Rock Rapid (slope = 0.025, elevation drop = 3.7 m), one of the steepest in Grand Canyon (Leopold 1969).

[5] We measured the rate of increase of O_2 concentration over the first 7 riffles and rapids downstream of Lees Ferry (Fig. 1A) 7 times from April 2007 to January 2009. Immediately prior to each survey, we calibrated a polarographic electrode or an optical dissolved oxygen sensor (Yellow Springs Instruments International, USA) in a 100-L pot filled with river water brought to dissolved O_2 saturation using an industrial aquarium bubbler. After calibration, we recorded dissolved oxygen readings for 0.5–1 h to both ensure minimal instrument drift and correct probe readings based on calculated saturation concentration (García and Gordon 1992). Following calibration we measured dissolved O_2 concentrations in the river above and below each rapid (Fig. 1). At each location, we measured O_2 and temperature at 20–30 points across the river by ferrying a motor boat along 2 transects from left bank to right bank and back again from right to left. Below House Rock Rapid, the end of the study reach, we checked calibration to correct measurements for probe

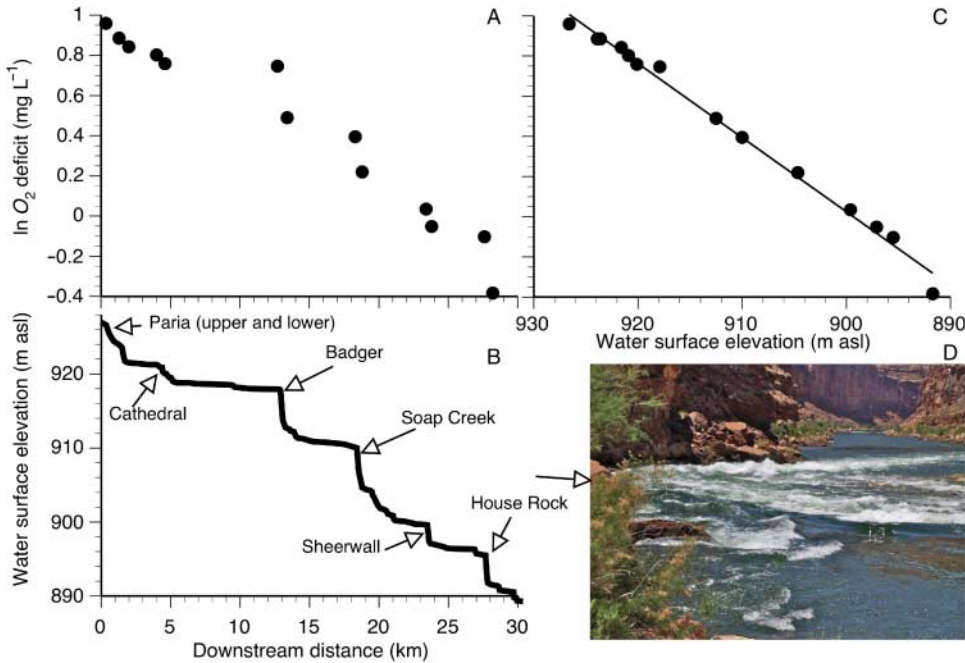


Fig. 1 A — Dissolved oxygen deficit ($\ln O_{2\text{def}}$) in the Colorado River declined downstream from Lees Ferry (km 0) on 27 June 2007. B — Water surface elevation measured by LIDAR over the 28-km study segment. The 7 study rapids are named. C — $\ln O_{2\text{def}}$ declined with water surface elevation (d). Line is a least-squares linear regression ($\ln O_{2\text{def}} = 0.0370d - 33.19$, $r^2 = 0.99$). D — House Rock Rapid looking downriver.

drift ($<0.2 \text{ mg O}_2 \text{ L}^{-1}$). Total time of each survey was roughly 2.5 h; the rate of change of O₂ concentrations during these brief surveys greatly exceeded that from biological metabolism, indicating changes in O₂ over our study reach were due primarily to air–water gas exchange (see Discussion).

[6] We calculated the morphology of rapids and the long reaches between them using high-resolution light detection and ranging (LIDAR) data on water surface elevations (Magirl et al. 2005). We estimated the elevation loss across rapids as the difference between elevation of the pool at the top of the rapid and the elevation below the rapid at which instantaneous measures of slope declined to 0.0005–0.001, which is 10–20 times lower than the average slope of rapids. Rapid length was the distance between the 2 elevation points, and slope (S) was elevation loss divided by rapid length. Mean width (w) of the study segment varied from 86 to 91 m, depending on discharge (Magirl et al. 2005). Discharge (Q) varied throughout the day because of dam operations, so we estimated discharge and velocity (v) at each site using a reach-averaged,

1-dimensional flow model (Graf 1995; Wiele and Smith 1996). The mean depth of the segment (z), based on continuity, that is, $z = Q (wv)^{-1}$, ranged from 4.3 to 4.7 m. All surveys occurred on rising discharge, and the speed at which we moved down the river was about as fast as the discharge wave. Hence, discharge varied $<10\%$ among sites within a survey.

[7] We converted O₂ concentrations to the saturation deficit ($O_{2\text{def}}$) at each location as

$$O_{2\text{def}} = O_{2\text{sat}} - O_2, \quad (1)$$

where O_2 is O₂ concentration (mg L^{-1}) and $O_{2\text{sat}}$ is the calculated saturation

concentration of O₂ based on temperature and measured barometric pressure (García and Gordon 1992).

[8] We modeled $O_{2\text{def}}$ downstream as a first-order rate where O₂ approaches saturation (i.e., $O_{2\text{def}} = 0$):

$$\frac{dO_{2\text{def}}}{dx} = -K_d O_{2\text{def}} \quad (2)$$

where x is the distance downstream (m) and K_d is the per-length exchange rate of oxygen. To estimate the value of K_d for a given river reach (i.e., a rapid or the reach between rapids) we used a 2-point estimate of K_d , where x is the length of the rapid or reach, fitted to the data using a solved Eq. 2:

$$\ln O_{2\text{def},x} = \ln O_{2\text{def},0} - K_d x \quad (3)$$

where $O_{2\text{def},0}$ and $O_{2\text{def},x}$ are O₂ saturation deficits at the top of a rapid and x m downstream, respectively. Gas transfer velocity for each reach (k_{O_2} , m min^{-1} or cm h^{-1}) is

$$k_{O_2} = \frac{QK_d}{w}. \quad (4)$$

[9] To estimate the gas exchange rate for the entire 28-km segment, we calculated the change in $O_{2\text{def}}$ with

respect to the change in water surface elevation (Fig. 1C):

$$\ln O_{2\text{def},d} = \ln O_{2\text{def},0} - K_{\text{drop}}d \quad (5)$$

where $O_{2\text{def},0}$ and $O_{2\text{def},d}$ are the oxygen saturation deficits at the top of the segment and d lower in water surface elevation (in m). K_{drop} is the per-unit length rate of oxygen change as a function of river elevation loss. We calculated K_{drop} by fitting Eq. 5 to the data using least-squares regression and solving for K_{drop} . Gas transfer velocity for the entire 28-km reach was calculated using Eq. 4, K_{drop} , and the mean slope of the segment. This calculation is equivalent to estimating K_d for the 28-km segment and k_{600} using Eq. 4. However, we need to estimate K_{drop} in order to scale gas exchange to unmeasured reaches. The per-time rate of O_2 exchange for the entire segment (K_r) is $k_{O_2}z^{-1}$ (where z is mean depth).

[10] Gas transfer velocity can be calculated for other temperatures (or other gases) based on the ratio of the Schmidt numbers (the dimensionless ratio of the kinematic viscosity and the diffusion coefficient, Sc) (Jahne et al. 1987):

$$\frac{k_{Sc_1}}{k_{Sc_2}} = \left(\frac{Sc_1}{Sc_2}\right)^{-1/2}. \quad (6)$$

We calculated Sc for O_2 at various temperatures following Wanninkhof (1992) and converted to Sc at 600 to compare with published gas exchange velocities. The exponent in Eq. 6 can range from -0.5 to -0.67 . We selected a value of -0.5 for the exponent because this is the value typically assumed for waves (Jahne et al. 1987; Wanninkhof 1992) and using other possible values has only a minor influence on k_{600} . For example, at 10°C , k_{600} calculated with an exponent of -0.67 was only 7.7% higher than that for -0.5 .

[11] We used least-squares linear regression to estimate the slope of the relationship between water surface elevation and $O_{2\text{def}}$. We calculated confidence intervals around mean rates assuming a t -distribution. To estimate the relationship between \log_{10} slope and $\log_{10} k_{600}$, we used standardized major axis (SMA) regression. This method minimizes variation in both x and y directions and estimates the linear relationship between symmetric variables (Warton et al. 2006). Five

of the 84 estimates of k_{600} were negative, so we assumed these reaches had k_{600} of 2 cm h^{-1} . We tested the effect of adding discharge to this linear model of $\log_{10} k_{600}$ versus \log_{10} slope by comparing the 2 models using Akaike's information criterion corrected for small sample size (AIC_c), which balances predictive ability and parsimony. Lower AIC_c indicates the best fit and AIC_c differences < 2 indicate equivalent models.

[12] We estimated Froude number (dimensionless ratio of water velocity to wave propagation velocity) as

$$Fr = \left(\frac{Q^2w}{gA^3}\right)^{1/2} \quad (7)$$

where g is the acceleration due to gravity and A (m^2) is the cross-sectional area of the rapid. This equation assumes 1-dimensional flow but provides a reasonable estimate of Fr given no knowledge of flow variation within these rapids (Magirl et al. 2009). We do not have bathymetric data for these rapids, and thus we calculated cross-sectional area A (m^2) from Manning's equation assuming perimeter \approx width as

$$A = \left(\frac{Qnw^{2/3}}{S^{1/2}}\right)^{3/5} \quad (8)$$

where n is Manning's roughness coefficient and S is slope. We assumed n for rapids was 0.08 based on boulder size in rapids (Lee 1989); this estimate is close to 0.06 assumed for Crystal Rapid (Kieffer 1985).

[13] An objective of this study was to scale gas exchange estimates to other reaches in the Colorado River for future segment-scale estimates of primary production (Odum 1956). Because the steep decline in $O_{2\text{def}}$ occurred only in the first 28 km of a 360-km reach, we needed to scale air–water gas exchange velocities to the rest of the river in Grand Canyon. Given the extreme spatial heterogeneity in gas transfer velocity (see Results), we need to consider over what segment length to estimate rates of k_{600} . We chose segment lengths that corresponded to 80% of the turnover distance of O_2 (Chapra and Di Toro 1991) because 80% balances assessing the majority of oxygen exchange with doubling reach length (necessary for 95% of exchange), which may bias estimates of gas exchange. Based on a

$K_{\text{drop O}_2}$ of 0.0425 m^{-1} at mean Q of $325 \text{ m}^3 \text{ s}^{-1}$, the downstream loss in elevation necessary to exchange 80% of the O₂ pool was 37.8 m. Using LIDAR data (Magirl et al. 2005), we calculated the distance upriver over which the river dropped 37.8 m at 10-km intervals throughout the entire 360-km river segment. We then calculated k_{O_2} for this segment based on combining Eq. 3 and Eq. 4:

$$k_{\text{O}_2} = \frac{-\ln(0.2)Q}{wx} \quad (9)$$

where k_{O_2} is the gas transfer velocity for oxygen at a mean temperature of 12 °C (average temperature during the 7 surveys) and w is the mean width for the segment of length x (mean length of all segments was $26.1 \text{ km} \pm 7.5$ [mean \pm SD]). We then converted k_{O_2} to k_{600} using Eq. 6.

Results

[14] Dissolved O₂ concentration in the Colorado River increased from an average of 72% saturation to 93% along the 28-km study segment (Fig. 1A). Areas of highest O₂ exchange occurred in the rapids that had large drops in elevation (Fig. 1A,B). Because rapids were unevenly spaced, $\ln O_{2\text{def}}$ did not decline linearly with distance downstream (Fig. 1A). In contrast, river water surface elevation linearly predicted $\ln O_{2\text{def}}$ (Fig. 1C). Surveys ended below House Rock Rapid because 93% was so close to saturation that small variation in measured O₂ led to large variation in $\ln O_{2\text{def}}$.

[15] Gas transfer velocity (k_{600}) increased as a function of river slope for both rapids and reaches between rapids (Fig. 2). Gas transfer velocity varied 4000-fold among reaches. Flat reaches between rapids (slope = 0.0003) had $k_{600} < 10 \text{ cm h}^{-1}$, whereas rapids had much higher k_{600} ; the steepest rapid, House Rock (slope = 0.025), ranged from 3600 to 7700 cm h^{-1} (Fig. 2). Using linear regression, \log_{10} of reach slope explained 89% variation in $\log_{10} k_{600}$ (Fig. 2). Thus, river slope explained a substantial fraction of variation in $\log_{10} k_{600}$ in the 28-km study segment. The model with slope alone had a lower AIC_c than the model with both slope and discharge, showing that incorporating discharge via multiple regression did not increase

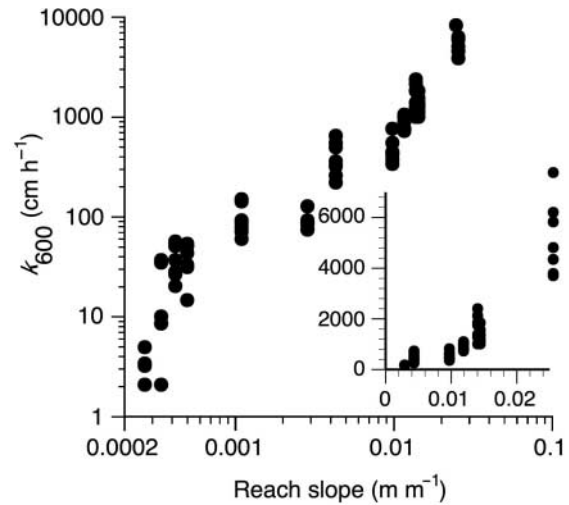


Fig. 2 Gas transfer velocity (k_{600} , cm h^{-1}) increased as a function of slope of a particular reach for each of the 7 surveys. Standardized major axis regression slope is 1.37 (95% CI: 1.27–1.47). Inset contains same data for the 7 study rapids plotted on an arithmetic scale.

prediction of k_{600} ($AIC_c = 49.9$ for a model with S only; $AIC_c = 52.1$ for model with $S + Q$). The value of the SMA regression slope between \log_{10} reach slope and $\log_{10} k_{600}$ was 1.37 (95% confidence interval [CI], 1.27–1.47), showing that as slope increased, gas transfer velocity increased at a proportionately higher rate (Fig. 2). Fr was also strongly positively related with $\log_{10} k_{600}$ for estimates in the 7 rapid reaches ($r^2 = 0.91$); however, this effect was mediated by slope because \log_{10} slope strongly predicted Fr ($r^2 = 0.97$).

[16] The per-meter drop in oxygen exchange rate ($K_{\text{drop } 600}$) averaged 0.048 m^{-1} across the 7 surveys and declined with increasing discharge (Fig. 3A). Gas transfer velocity (k_{600}) between Lees Ferry and House Rock Rapid averaged 86.6 cm h^{-1} (95% t -based CI, 76–95 cm h^{-1} ; range, 74–101 cm h^{-1}) and varied little among surveys; that is, coefficient of variation (CV) was 11%. Gas transfer velocity was calculated using discharge; hence, we cannot evaluate a statistical relationship between the two. However, we can compare among scenarios to show how Q relates with gas transfer velocity. For example, if the fraction of decline of K_{drop} equaled the increase in Q , then gas transfer velocity would increase steeply. If mechanisms driving gas exchange stayed the same among discharges, then gas transfer velocity would be constant. The relationship between gas transfer velocity and Q was between

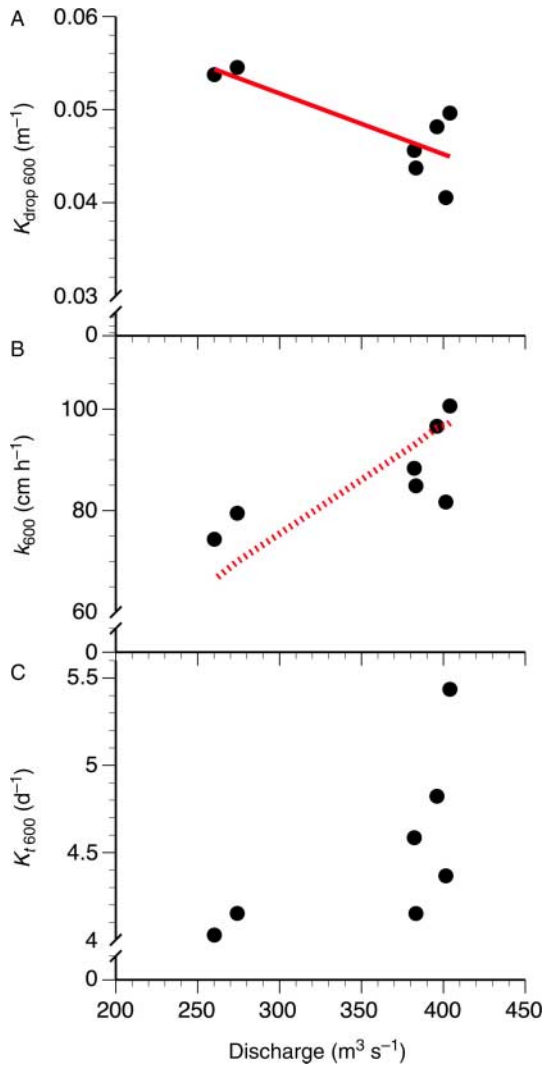


Fig. 3 A — Rate of gas exchange (per-unit length elevation drop, scaled to a Schmidt number of 600 [$S_{C_{600}}$]) declined with increasing discharge (Q , $m^3 s^{-1}$). Each point represents a segment-scale estimate from 1 of 7 surveys. Line is least-squares linear regression ($K_{drop\ 600} = -6.53 \times 10^{-5}Q + 0.071$, $r^2 = 0.63$, $p = 0.033$). B — Gas transfer velocity (k_{600} , $cm\ h^{-1}$) increased with river discharge. Dotted line is predicted gas transfer velocity if K_{drop} were constant with discharge. C — Per-unit time rate of gas exchange ($K_{t\ 600}$, d^{-1}) was unrelated to Q (linear regression, $\rho = 0.12$).

these 2 extremes (Fig. 3B). In contrast, gas exchange as a per-unit time rate ($K_{t\ 600}$) averaged $4.5\ d^{-1}$ (95% CI, 4.04–4.96 d^{-1}), varied little among surveys (CV = 11%), and was unrelated to discharge (Fig. 3C).

[17] At the scale of river segments corresponding to 80% of the oxygen turnover (mean length = 26.1 km; range, 13.4–41.7 km), k_{600} varied from 56 to 272 $cm\ h^{-1}$ throughout Grand Canyon (Fig. 4). The high value was

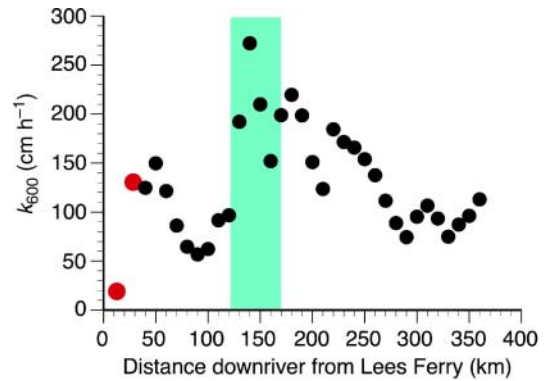


Fig. 4 Scaled estimates of gas transfer velocity (k_{600} , $cm\ h^{-1}$) varied strongly along the Grand Canyon segment of the Colorado River. Red circles are measured rates from Lees Ferry to above Badger Creek Rapid and from Badger Creek Rapid to below House Rock Rapid. Filled circles are modeled estimates of k_{600} . The green shading from 120 to 170 km represents the Upper Granite Gorge, which extends from Hance Rapid to Serpentine Rapid. This segment contains many of the largest rapids in Grand Canyon.

from the reach extending from Hance Rapid to Bright Angel Creek, which is the beginning of the Upper Granite Gorge (Schmidt and Graf 1990) and one of the steepest reaches in Grand Canyon. The canyon-wide mean k_{600} was $113\ cm\ h^{-1}$.

Discussion

Controls on k_{600}

[18] The downstream decline in O_{2def} reflected high rates of gas exchange within rapids along a 28-km river segment of the Colorado River. Gas transfer velocity varied spatially, with high rates in rapids and low rates in quiescent reaches between rapids. High rates of gas exchange in this whitewater river were not unexpected. An extensive engineering literature shows how isolated control structures (e.g., low-head dams, grates, and weirs) strongly aerate water at discrete locations (Avery and Novak 1978; Gulliver et al. 1998; Caplow et al. 2004). Alternatively, tracer and dome techniques show how wind, bottom-induced turbulence, and geomorphology regulate gas exchange over larger spatial scales (Cole and Caraco 1998; Melching and Flores 1999; Borges et al. 2004). Here we have combined these 2 approaches, that is, measuring controls on gas exchange in rapids and then estimating a rate for a 28-km segment.

[19] For the purposes of measuring gas exchange in Grand Canyon, the large hypolimnetic release dam

immediately upstream released low-O₂ water that provided conditions analogous to a tracer addition. In lower canyon reaches, O₂ slightly exceeded saturation and there was no measurable change across rapids. Other rivers with dams or discontinuities that lower O₂ or other gases substantially below atmospheric saturation may apply our approach to measure gas transfer velocity. One consideration, however, is that change in gas concentration must be primarily due to gas exchange rather than biological or chemical processes. We can test this assumption for our study reach because we have seasonal diel O₂ data for a site 20 km below House Rock Rapid. Rate of change of O₂ in the morning, which is when primary production increased most quickly, averaged 0.029 mg O₂ L⁻¹ h⁻¹ ($n = 6$). Rate of change in O₂ during our 2.5-h survey was 0.75 mg O₂ L⁻¹ h⁻¹ ($n = 7$). Thus, the change in O₂ from air–water gas exchange exceeded that from biological productivity 25-fold, allowing us to use this O₂ change to estimate gas exchange accurately.

[20] For short river reaches, that is, the lengths of rapids or the reaches between them, river slope strongly regulated k_{600} . Empirical analyses of gas exchange in streams and rivers show that the per-unit time rate of gas exchange (K_t) increases with increasing slope (Melching and Flores 1999). Slope is related to several physical mechanisms that regulate gas exchange. Steeper slopes increase water velocity and therefore turbulence, which is directly related to oxygen exchange (Borges et al. 2004; Zappa et al. 2007). In rapids, turbulence increases to the point where the water surface breaks and air bubbles are advected into the flow, greatly increasing gas transfer velocity. The relationship between reach slope and k_{600} was nonlinear, with k_{600} increasing faster than slope, suggesting that turbulence and bubble formation also increase nonlinearly with reach slope. This finding is similar to ocean gas exchange, where k_{600} increases as a cubic function of wind speed because of bubble enhancement of gas exchange, (McNeil and D'Asaro 2007; Wanninkhof et al. 2009). Bubbles can dramatically increase gas transfer velocity (Wanninkhof et al. 2009), though the fractional transfer velocity for bubbles is unknown in oceans. Like windy oceans, bubble formation in rapids is likely the dominant mechanism of gas exchange, thus allowing for dramatically

higher rates of k_{600} relative to flat reaches. The extreme turbulence in rapids and subsequent bubble formation is likely what drove gas transfer velocity (up to 7700 cm h⁻¹) that greatly exceeded estimates for virtually all other types of aquatic ecosystems.

[21] Gas exchange via bubbles complicates simple models of gas exchange. One complication is that gas invasion is faster than evasion because bubbles are under pressure relative to the atmosphere (Keeling 1993). Thus, differences in partial pressure between water and air will not be directly proportional to gas flux. Supersaturation of gas in water provides evidence for this phenomenon (Keeling 1993), which occurs for O₂ in the Colorado River (R. O. Hall, unpublished data). Oxygen is poorly suited to accurately estimate the degree of oversaturation (and thus the effect of bubbles on gas exchange) because photosynthesis and respiration regulate concentrations, along with air–water exchange. However, if photosynthesis is low and O₂ is supersaturated despite respiration, then there is evidence of bubble formation oversaturating concentrations. As part of a 2-year study on measuring metabolism at a site 360 km downriver from Lees Ferry, we have measured oxygen concentrations continually. During the period 24 July to 9 August 2010, we observed no measurable photosynthesis due to exceptionally high water turbidity (R. O. Hall et al., unpublished data). Mean daily concentrations ($n = 288$ O₂ measurements each day) during this period ranged from 97.8% to 101.8% despite ongoing respiration. Thus, we observed oxygen concentrations above saturation when photosynthesis is zero, showing that bubble formation is a large component of gas exchange.

[22] A second complication of bubble-driven gas exchange is that transfer velocity will depend on the solubility of gases as well as the diffusivity, and simple scaling among gases by the ratio of the Schmidt numbers (Eq. 6) is not valid (Asher et al. 1997; Asher and Wanninkhof 1998). Here we used oxygen to parameterize models of oxygen exchange, and thus the bias of using Schmidt number scaling among temperatures should be low. These gas transfer velocities should be used with caution to examine, for example, exchange of CO₂, which is much more soluble than O₂. If we had used a deliberate tracer gas, such as SF₆, scaling to O₂

would have been more uncertain. The role of bubbles in gas exchange represents an intense area of research in oceans (Asher and Wanninkhof 1998). It is likely that bubbles drive gas exchange in high-energy streams and rivers, that is, those with white water sections. Outside of well-developed data and modeling for spillways (Wilhelms and Gulliver 2005a, 2005b), little is known about bubble-driven gas exchange for whitewater rivers.

[23] Pinpointing the within-rapid hydraulic mechanisms that regulate gas exchange in a Colorado River rapid will be difficult because there has been little research into the hydraulics of these rapids. Direct measurements of water velocity in rapids of the Colorado River were only recently made in Cataract Canyon, Utah (several hundred kilometers upriver of Grand Canyon) and documented that sections of rapids with higher slopes have higher Fr (Magirl et al. 2009). Fr can predict gas exchange over control structures (Gulliver et al. 1998), and indeed, whole-rapid Fr predicted k_{600} in Grand Canyon, but Fr was simply a function of reach slope. It is difficult to measure hydraulic attributes of a big rapid given that simply controlling a boat is impossible in many parts of big rapids. Other than slope and width of the entire rapid, which are easily measured, much of the distinction among Grand Canyon rapids concerns their navigability. Stevens (1990) used a 10-point scale for rating the navigability of different rapids, with 10 being the most difficult. Interestingly, difficulty ratings for rapids correlated strongly and positively with $\log_{10} k_{600}$ ($r = 0.91$, $p = 0.012$, $n = 6$). Hydraulic jumps (“holes”), rocks, and waves impede navigation, and these features likely also drive gas exchange. House Rock Rapid (difficulty = 7; Stevens 1990) has 2 large hydraulic jumps through which much of the river flows, and these jumps likely cause most bubble formation and gas exchange in this rapid.

[24] River control structures can have high rates of gas exchange because they form bubbles to the extent where a large fraction of the water volume includes entrained air (Wilhelms and Gulliver 2005a). Individual control structures can turn over a substantial fraction of O_2 . Fraction exchange on a spillway in the Kost River, Minnesota, ranged between 0.01 and 0.24 (Wilhelms and Gulliver 2005b). Converting fraction exchanged to a gas transfer velocity gave mean k_{600} of 4800 cm h^{-1} ,

similar to big Colorado River rapids. A tracer gas study found that as the Hudson River passed over 2 low-head dams (5 and 6 m high), 72% of the SF_6 tracer was exchanged with the atmosphere (Caplow et al. 2004). This fraction is similar to our estimates of O_2 exchanged in the entire 28-km segment of the Colorado, indicating that these dams have higher ability to aerate water than rapids, undoubtedly because the total drop exceeded that of even the biggest Grand Canyon rapids.

Scaling and Comparing k_{600}

[25] The instantaneous rates of gas exchange in rapids and the reaches between them are not easily scaled to the entire 28-km segment because (1) it is necessary to know the amount of time water spends in each pool-rapid reach—these data do not exist for Grand Canyon and only exist for a few rapids in Cataract Canyon (Magirl et al. 2009)—and (2) we used \log_{10} scaled data in a linear regression to examine the relationship between river slope and k_{600} (Fig. 2). This log–log relationship had high uncertainty for the purposes of predicting k_{600} , and arithmetic-scaled data had very high variability (Fig. 2, inset). Because of the variable distance between rapids, the relationship between $\ln O_{2\text{def}}$ and distance was nonlinear and not easily scaled to downstream segments. Water surface elevation, on the other hand, related linearly with $\ln O_{2\text{def}}$ and allowed scaling of k_{600} to unmeasured downstream segments. This gas transfer velocity varied little with discharge, likely because higher discharge submerges rapids, thereby decreasing their slope, but this effect was balanced by increased stream power due to higher Q .

[26] Scaled estimates of k_{600} varied 4.5-fold throughout the 360 km Grand Canyon. The length of river chosen to estimate gas exchange will affect variability, with very short reaches (e.g., 1-km rapid or pool) having high variability (Fig. 2), whereas very long segments (e.g., 100 km) should have lower variability (Fig. 4). For our purposes—estimating rates of ecosystem metabolism using rate of change in O_2 —the appropriate length to scale k_{600} corresponds to the turnover distance of O_2 , an average of 26.1 km based on distance required to exchange 80% of O_2 . Geomorphic variability at the spatial scale of tens of kilometers regulates gas exchange, for example, steep segments through the

Upper Granite Gorge (120–170 km downstream from Lees Ferry) versus shallow sections in lower Marble Canyon (80–100 km downstream).

[27] Most estimates of k_{600} from rivers, estuaries, and oceans are lower than the river-wide estimate of 113 cm h^{-1} for the Colorado River, and no published estimates approach the k_{600} measured within rapids (Table 1). Ecosystems where wind regulates turbulence, such as lakes and oceans, have variable k_{600} ranging from low to high during extreme wind speeds during a hurricane (Wanninkhof et al. 2009; McNeil and D'Asaro 2007). This hurricane-induced gas transfer velocity was about 6 times higher than that for the Colorado River, but about 10 times lower than the highest value measured in House Rock Rapid. Gas exchange velocities for estuaries (Raymond and Cole 2001; Borges et al. 2004) were lower than that for the Colorado River, whereas k_{600} for low-slope rivers matched that for runs between rapids in Grand Canyon (Alin et al. 2011). Streams often have high k_{600} because of strong turbulence and bubble formation; however, most of the 380 streams had lower higher k_{O_2} than what we report here (Melching and Flores 1999). The Colorado River, because of high turbulence in rapids, had higher rates of gas exchange than those from most other ecosystems, including small streams.

Significance to Aquatic Environments

[28] Gas exchange can be highly spatially variable within a river. Gas transfer velocity for the Colorado River varied roughly 4000-fold among short reaches and 4-fold at the 13- to 42-km-segment scale. Thus k_{600} depended on the spatial scale of interest. Most estimates of k_{600} for rivers report a mean value with some uncertainty estimate, but this value may depend on the spatial scale, for example, a reach length from a tracer experiment versus distance of a dome float. Dome estimates are likely to be more robust when small-spatial-scale variability is minor. Tracer estimates can incorporate small-scale variability if sampling frequency is high, but tracers usually provide a segment-scale estimate of gas exchange corresponding to roughly the travel distance of the gas.

[29] Estimating and scaling k_{600} for rivers like the Colorado will enable more accurate estimates of gas fluxes from rivers to estimate ecosystem metabolism. Knowing these fluxes will allow ecologists to more accurately consider the role of rivers in continental element cycling (Cole et al. 2007; Beaulieu et al. 2011). In addition, rivers such as the Colorado with high gas exchange below hypolimnetic release reservoirs can effectively transfer trapped gases such as N₂O and methane from the hypolimnion to the atmosphere over a relatively short distance. The Colorado River is unlike most

Table 1 Gas exchange velocities (k_{600}) for different ecosystems. This list is not exhaustive; rather, it provides a range of values to compare with those from the Colorado River.

Ecosystem	k_{600} (cm h ⁻¹)		Reference
	Mean ± SD	Upper range	
Ocean-tracer studies	14 ^a	95	Wanninkhof et al. (2009)
Ocean during hurricane	376	620	McNeil and D'Asaro (2007)
Estuaries and rivers	6.6 ± 3.4	13	Raymond and Cole (2001)
Estuaries	24 ^b	50	Borges et al. (2004)
Streams in U.S.	18 ± 18	49 ^c	Melching and Flores (1999)
Lowland rivers > 100 m wide	15 ± 9	45	Alin et al. (2011)
Lowland rivers < 100 m wide	23 ± 17	71	Alin et al. (2011)
Streams, Wyoming	24 ± 18	42	Hall and Tank (2003)
Colorado River, rapids	1410 ± 1700	7730	Present study
Colorado River, runs	37 ± 36	143	Present study
Colorado River, entire river	113 ± 47	272	Present study

^aNormalized for wind speed of 8 m s^{-1} .

^bNormalized for wind speed of 6 m s^{-1} .

^c95% quantile of k_{O_2} ; temperature data were not available to convert to k_{600} .

well-studied rivers because of its large size and formidable rapids, yet it is not necessarily unique. Many rivers draining mountainous regions have high discharge and steep slopes resulting in large rapids. Many rivers also have low-head dams representing zones of high rates of gas exchange between low-exchange, impounded reaches. Rapid-filled reaches or low-head dams may be hot spots of gas efflux to the atmosphere because the timescale of gas exchange can far exceed water residence time. Our approach of measuring gas exchange at the scale of individual rapids (to provide mechanism), combined with segment-scale estimates, provides a means to measure and scale gas exchange to long stretches of river over a range of hydraulic conditions. Certainly k_{600} measured here will differ in other large rivers; however, measuring gas exchange in other rivers may lead to the development of more accurate predictive models of gas exchange at a range of spatial scales.

Acknowledgments Adam Copp and Trista Niekum helped in the field. Mike Yard, Brian Dierker, Brent Berger, and Scott Perry boated us safely through big rapids. Chris Magirl provided geomorphology data and clarified our thinking about rapids. Chris Magirl, Scott Wright, Jon Cole, and 2 anonymous reviewers commented on earlier drafts of the manuscript. Charles Melching provided data from their paper. Cooperative Agreement 05WRAG0055 through the U.S. Geological Survey and U.S. Bureau of Reclamation funded this study. Any use of trade, product, or firm names is for descriptive purposes only and does not imply endorsement by the U.S. government.

References

- Alin, S. R., M. F. F. L. Rasera, C. I. Salimon, J. E. Richey, G. W. Holtgrieve, A. V. Krusche, and A. Snidvongs. 2011. Physical controls on carbon dioxide transfer velocity and flux in low-gradient river systems and implication for regional carbon budgets. *J. Geophys. Res.* **116**: G01009, doi:10.1029/2010JG001398.
- Asher, W., and R. Wanninkhof. 1998. Transient tracers and air-sea gas transfer. *J. Geophys. Res.* **103**: 15939–15958, doi:10.1029/98JC00379.
- Asher, W. E., L. M. Karle, and B. J. Higgins. 1997. On the difference between bubble-mediated air-water transfer in freshwater and seawater. *J. Mar. Res.* **55**: 813–845, doi:10.1357/0022240973224210.
- Avery, S. T., and P. Novak. 1978. Oxygen transfer at hydraulic structures. *J. Hydraul. Div., Am. Soc. Civ. Eng.* **104**: 1521–1540.
- Beaulieu, J. J., et al. 2011. Nitrous oxide emission from denitrification in stream networks. *Proc. Natl. Acad. Sci. USA.* **108**: 214–219, doi:10.1073/pnas.1011464108.
- Borges, A. V., B. Delille, L.-S. Schiettecatte, F. Gazeau, G. Abril, and M. Frankignoulle. 2004. Gas transfer velocities of CO₂ in three European estuaries (Randers Fjord, Scheldt, and Thames). *Limnol. Oceanogr.* **49**: 1630–1641, doi:10.4319/lo.2004.49.5.1630.
- Caplow, T., P. Schlosser, and D. T. Ho. 2004. Tracer study of mixing and transport in the upper Hudson River with multiple dams. *J. Environ. Eng.* **130**: 1498–1506, doi:10.1061/(ASCE)0733-9372(2004)130:12(1498).
- Chapra, S. C., and D. M. DiToro. 1991. Delta method for estimating primary production, respiration and reaeration in streams. *J. Environ. Eng.* **117**: 640–655, doi:10.1061/(ASCE)0733-9372(1991)117:5(640).
- Clark, J. F., R. Wanninkhof, P. Schlosser, and H. J. Simpson. 1994. Gas exchange rates in the tidal Hudson River using a dual tracer technique. *Tellus, Ser. B.* **46**: 274–285, doi:10.1034/j.1600-0889.1994.t01-2-00003.x.
- Cole, J. J., et al. 2007. Plumbing the global carbon cycle: Integrating inland waters into the terrestrial carbon budget. *Ecosystems* **10**: 172–185, doi:10.1007/s10021-006-9013-8.
- Cole, J. J., and N. F. Caraco. 1998. Atmospheric exchange of carbon dioxide in a low-wind oligotrophic lake. *Limnol. Oceanogr.* **43**: 647–656, doi:10.4319/lo.1998.43.4.0647.
- Dolan, R., A. Howard, and D. Trimble. 1978. Structural control of the rapids and pools of the Colorado River in the Grand Canyon. *Science* **202**: 629–631, doi:10.1126/science.202.4368.629.
- García, H. E., and L. I. Gordon. 1992. Oxygen solubility in seawater: Better fitting equations. *Limnol. Oceanogr.* **37**: 1307–1312, doi:10.4319/lo.1992.37.6.1307.
- Graf, J. B. 1995. Measured and predicted velocity and longitudinal dispersion at steady and unsteady flow, Colorado River, Glen Canyon to Lake Mead. *Water Resour. Bull.* **31**: 265–281.
- Gulliver, J. S., S. C. Wilhelms, and K. L. Parkhill. 1998. Predictive capabilities in oxygen transfer at hydraulic structures. *J. Hydraul. Eng.* **124**: 664–671, doi:10.1061/(ASCE)0733-9429(1998)124:7(664).
- Hall, R. O., and J. L. Tank. 2003. Ecosystem metabolism controls nitrogen uptake in streams in Grand Teton National Park, Wyoming. *Limnol. Oceanogr.* **48**: 1120–1128, doi:10.4319/lo.2003.48.3.1120.
- Ho, D. T., P. Schlosser, and P. M. Orton. 2011. On factors controlling air-water gas exchange in a large tidal river. *Estuaries Coasts.* **34**: 1103–1116, doi:10.1007/s12237-011-9396-4.
- Jahne, B., K. O. Munnich, R. Bosinger, A. Dutzi, and W. Huber. 1987. On parameters influencing air-water gas exchange. *J. Geophys. Res.* **74**: 456–464.
- Keeling, R. F. 1993. On the role of large bubbles in air-sea gas exchange and supersaturation in the ocean. *J. Mar. Res.* **51**: 237–271, doi:10.1357/0022240933223800.
- Kieffer, S. W. 1985. The 1983 hydraulic jump in Crystal Rapid: Implications for river running and geomorphic evolution in the Grand Canyon. *J. Geol.* **93**: 385–406, doi:10.1086/628962.

- Kremer, J. N., S. W. Nixon, B. Buckley, and P. Roques. 2003. Technical note: Conditions for using the floating chamber method to estimate air–water gas exchange. *Estuaries*. **26**: 985–990, doi:10.1007/BF02803357.
- Lee, S. E. 1989. The effect of Glen Canyon Dam on the stability of rapids in the Colorado River, Grand Canyon, Arizona. M.S. thesis, Arizona State University.
- Leopold, L. B. 1969. The rapids and the pools—Grand Canyon. Geological Survey Professional Paper 669-D.
- Magirl, C. S., J. W. Gartner, G. M. Smart, and R. H. Webb. 2009. Water velocity and the nature of critical flow in large rapids on the Colorado River, Utah. *Water Resour. Res.* **45**: W05427, doi:10.1029/2009WR007731.
- Magirl, C. S., R. H. Webb, and P. G. Griffiths. 2005. Changes in the water surface profile of the Colorado River in Grand Canyon, Arizona, between 1923 and 2000. *Water Resour. Res.* **41**: W05021, doi:10.1029/2003WR002519.
- Marino, R., and R. W. Howarth. 1993. Atmospheric oxygen exchange in the Hudson River: Dome measurements an comparison with other natural waters. *Estuaries Coasts* **16**: 433–455, doi:10.2307/1352591.
- McNeil, C., and E. D'Asaro. 2007. Parameterization of air–sea gas fluxes at extreme wind speeds. *J. Mar. Syst.* **66**: 110–121, doi:10.1016/j.jmarsys.2006.05.013.
- Melching, C. S., and H. E. Flores. 1999. Reaeration equations derived from U.S. Geological Survey database. *J. Environ. Eng.* **125**: 407–414, doi:10.1061/(ASCE)0733-9372(1999)125:5(407).
- Mulholland, P. J., et al. 2001. Inter-biome comparison of factors controlling stream metabolism. *Freshw. Biol.* **46**: 1503–1517, doi:10.1046/j.1365-2427.2001.00773.x.
- Odum, H. T. 1956. Primary production in flowing waters. *Limnol. Oceanogr.* **1**: 102–117, doi:10.4319/lo.1956.1.2.0102.
- Raymond, P. A., and J. J. Cole. 2001. Gas exchange in rivers and estuaries: Choosing a gas transfer velocity. *Estuaries Coasts* **24**: 312–317, doi:10.2307/1352954.
- Schmidt, J. C., and J. B. Graf. 1990. Aggradation and degradation of alluvial sand deposits, 1965 to 1986, Colorado River, Grand Canyon National Park, Arizona. U.S. Geological Survey Professional Paper 1493.
- Stevens, L. 1990. The Colorado River in Grand Canyon—a comprehensive guide to its natural and human history. Red Lake Books.
- Wanninkhof, R. 1992. Relationship between wind speed and gas exchange over the ocean. *J. Geophys. Res.* **97**: 7373–7382, doi:10.1029/92JC00188.
- Wanninkhof, R., W. Asher, R. Wepperling, H. Chen, P. Schlosser, C. Langdon, and R. Sambretto. 1993. Gas transfer experiment on Georges Bank using two volatile deliberate tracers. *J. Geophys. Res.* **98**: 20237–20248, doi:10.1029/93JC01844.
- Wanninkhof, R., W. E. Asher, D. T. Ho, C. S. Sweeney, and W. R. McGillis. 2009. Advances in quantifying air–sea gas exchange and environmental forcing. *Annu. Rev. Mar. Sci.* **1**: 213–244, doi:10.1146/annurev.marine.010908.163742.
- Wanninkhof, R., P. J. Mulholland, and J. W. Elwood. 1990. Gas exchange rates for a first-order stream determined with deliberate and natural tracers. *Water Resour. Res.* **26**: 1621–1630.
- Warton, D. I., I. J. Wright, D. S. Falster, and M. Westoby. 2006. Bivariate line-fitting methods for allometry. *Biol. Rev. Camb. Philos. Soc.* **81**: 259–291, doi:10.1017/S1464793106007007.
- Wiele, S. M., and J. D. Smith. 1996. A reach-averaged model of diurnal discharge wave propagation down the Colorado River through the Grand Canyon. *Water Resour. Res.* **32**: 1375–1386, doi:10.1029/96WR00199.
- Wilhelms, S. C., and J. S. Gulliver. 2005a. Bubbles and waves description of self-aerated spillway flow. *J. Hydraul. Res.* **43**: 522–531, doi:10.1080/00221680509500150.
- Wilhelms, S. C., and J. S. Gulliver. 2005b. Gas transfer, cavitation, and bulking in self-aerated spillway flow. *J. Hydraul. Res.* **43**: 532–539, doi:10.1080/00221680509500151.
- Zappa, C. J., W. R. McGillis, P. A. Raymond, J. B. Edson, E. J. Hinst, H. J. Zemelink, J. W. H. Dacey, and D. T. Ho. 2007. Environmental turbulent mixing controls on air–water gas exchange in marine and aquatic systems. *Geophys. Res. Lett.* **34**: L10601, doi:10.1029/2006GL028790.

Received: 23 February 2011

Amended: 25 October 2011

Accepted: 2 January 2012